

Supporting Information

Investigation on Heat Transfer in a Semicrystalline Polymer by Combining Molecular Simulations and Machine Learning

Zoumeng Hu¹, Chen Jia¹, Yonglai Lu¹, Jingchao Li³, Ruibin Ma⁴, Xiuying Zhao¹, Liquan Zhang¹, Jihua Zhang^{2*}, Yangyang Gao^{1*}

¹Key Laboratory of Beijing City on Preparation and Processing of Novel Polymer Materials, Beijing University of Chemical Technology, Beijing 10029, People's Republic of China

²Aerospace Research Institute of Materials and Processing Technology, Beijing, 100076, People's Republic of China

³Beijing Key Laboratory of Wood Science and Engineering, Beijing Forestry University, Beijing 100083, People's Republic of China

⁴Institute of Intelligent Innovation, Henan Academy of Sciences, Zhengzhou, 451162, People's Republic of China

*Corresponding author: Email: gaoyy@mail.buct.edu.cn

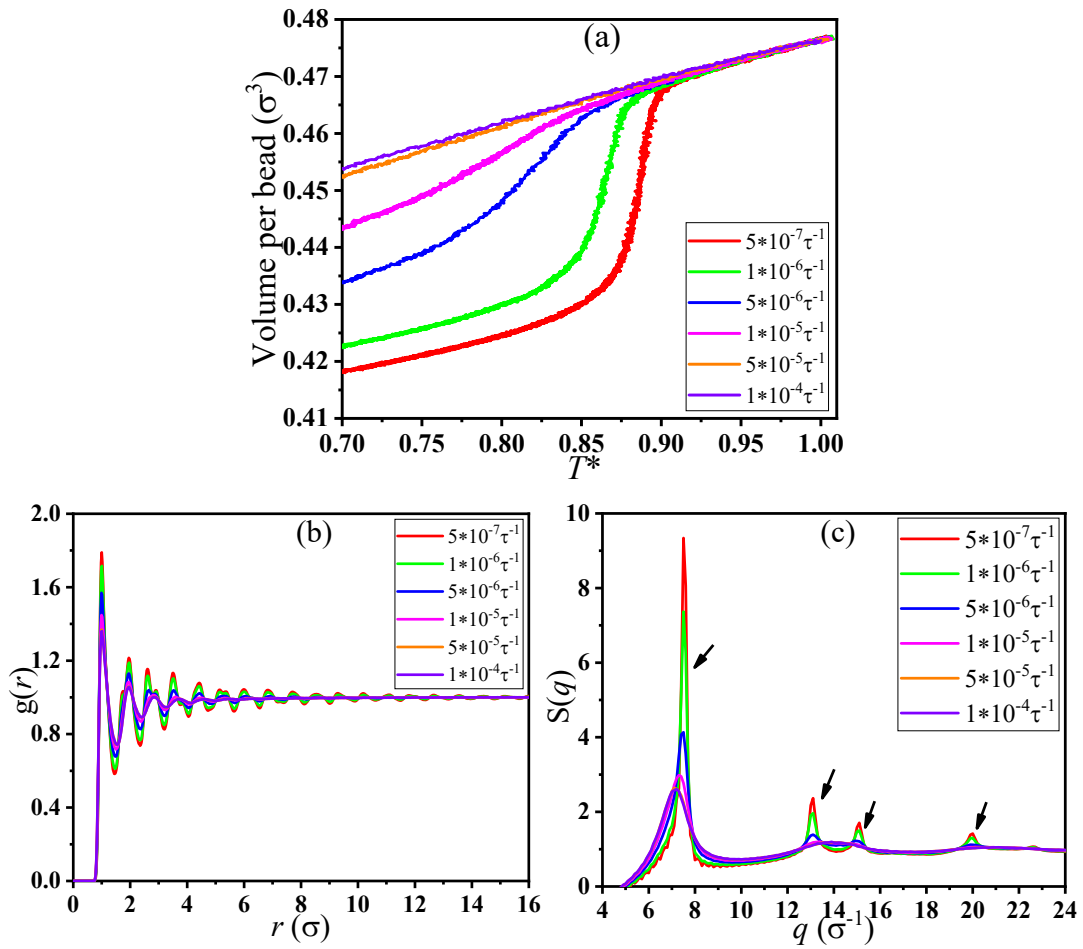


Figure S1. (a) The volume per bead with the temperature T^* , (b) radial distribution function $g(r)$ and (c) static structure factor $S(q)$ at different cooling rates.

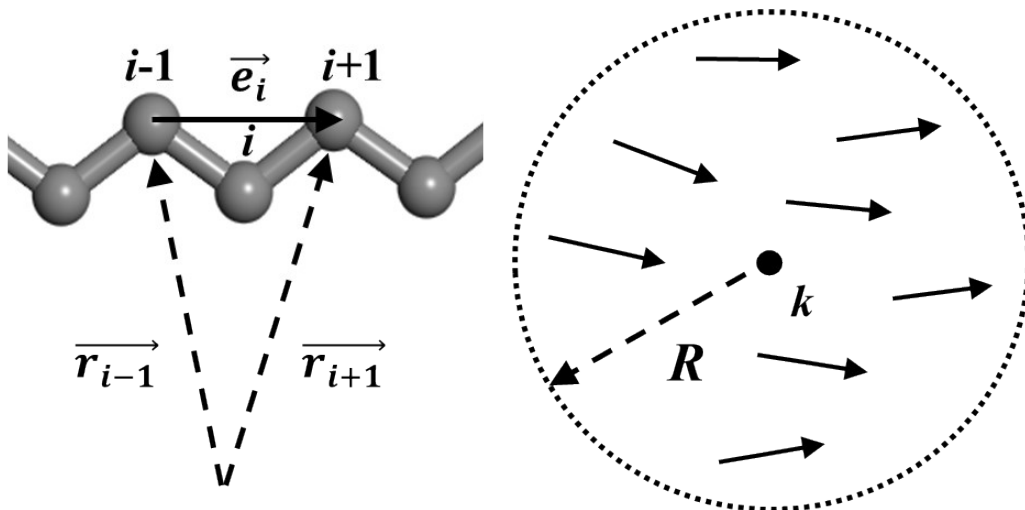


Figure S2. The unit vector of bead i and local order parameter of model.

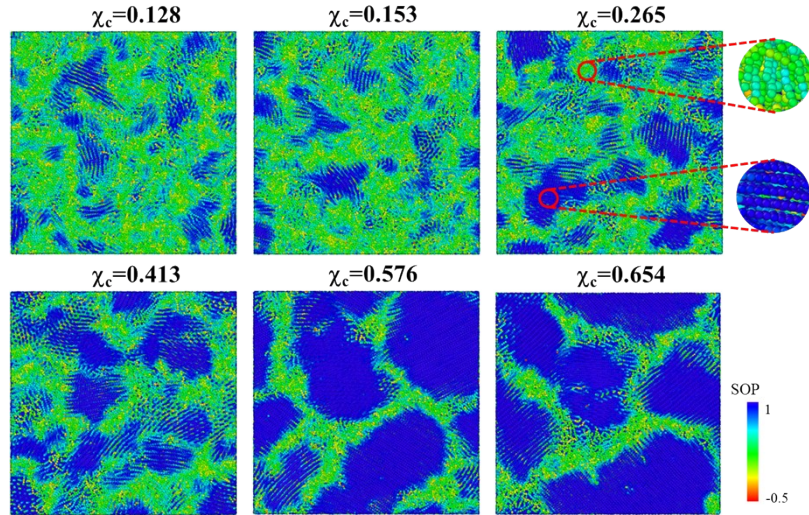


Figure S3. Diagrams of the semicrystalline polymer with different crystallinities χ_c .

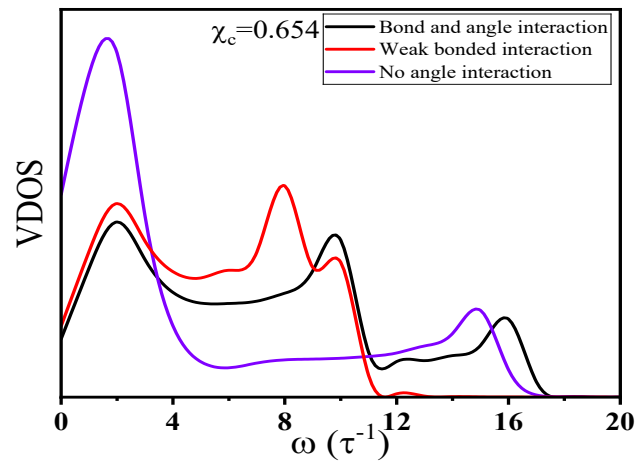


Figure S4. The vibrational density of states (VDOS) of semicrystalline polymer at crystallinity $\chi_c = 0.654$ and two additional models with weak bonded interaction or no angle interaction.

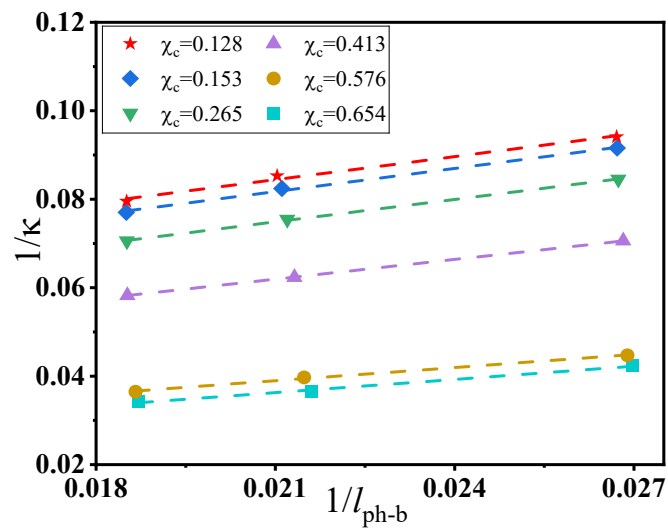


Figure S5. The $1/\kappa$ vs $1/l_{\text{ph-b}}$ curves for different crystallinities χ_c .

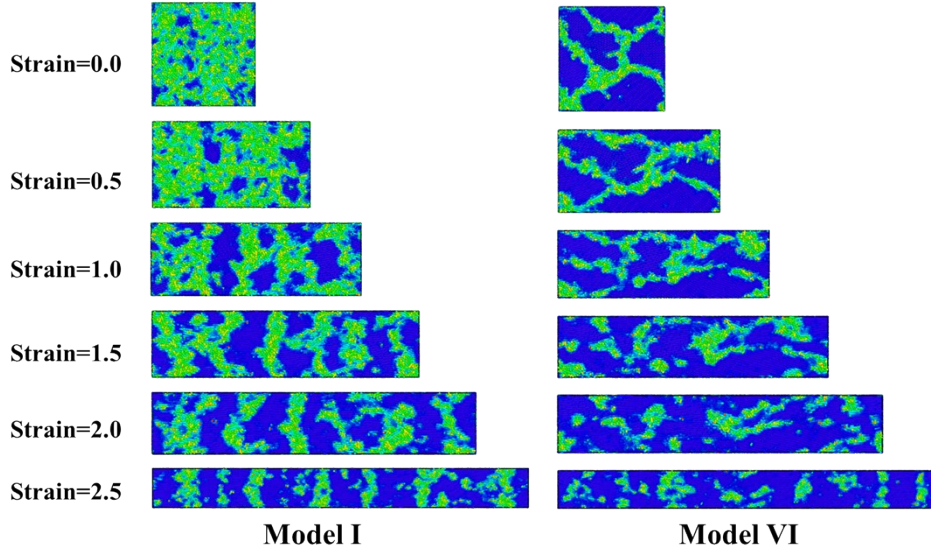


Figure S6. Diagrams of the semicrystalline polymer as a function of strain for model I ($\chi_c = 0.128$) and model VI ($\chi_c = 0.654$).

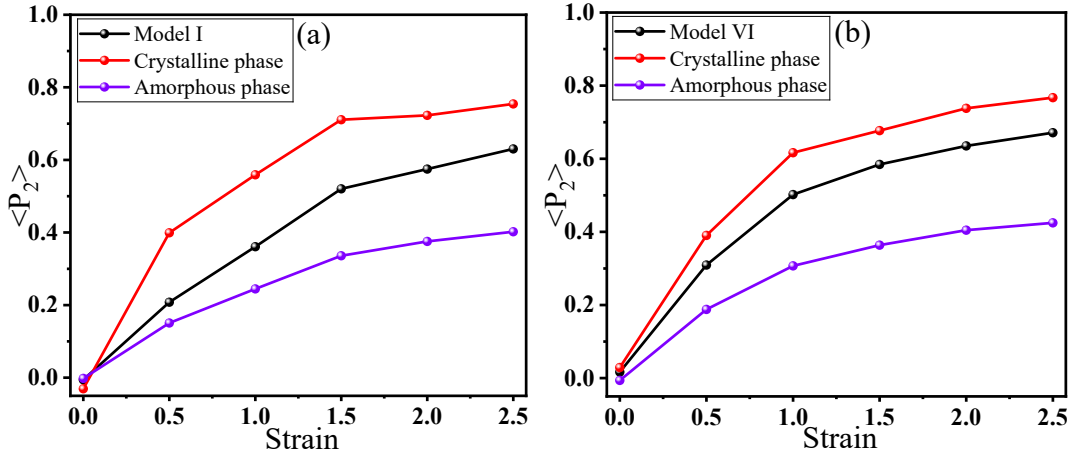


Figure S7. The orientation degree of chains ($\langle P_2 \rangle$) as a function of strain for (a) model I ($\chi_c = 0.128$) and (b) model VI ($\chi_c = 0.654$).

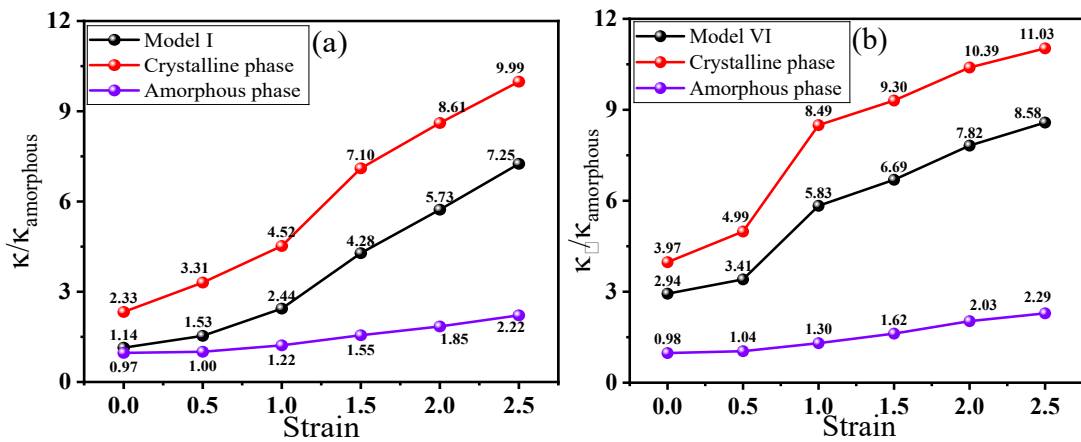


Figure S8. Thermal conductivity ratio ($\kappa/\kappa_{amorphous}$) of the crystalline or amorphous phases as a function of strain for (a) model I ($\chi_c = 0.128$) and (b) model VI ($\chi_c = 0.654$).

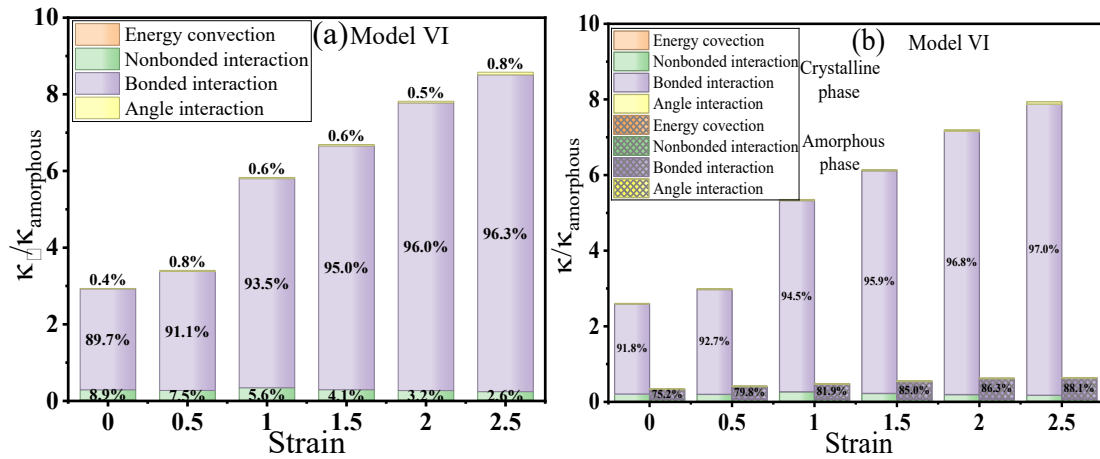


Figure S9. Contributions by four energy transfer modes (energy convection, nonbonded interaction, bonded interaction and angle interaction) (a) in the semicrystalline polymer (b) in the crystalline or amorphous phases for model VI ($\chi_c = 0.654$).

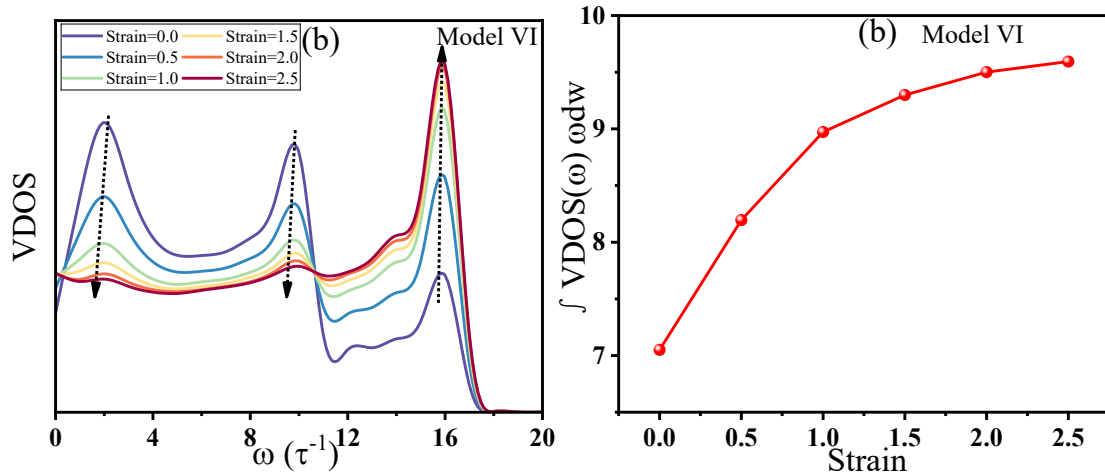


Figure S10. (a) The vibrational density of states (VDOS) of semicrystalline polymer and (b) $\int \text{VDOS}(\omega) \omega d\omega$ for model VI ($\chi_c = 0.654$).

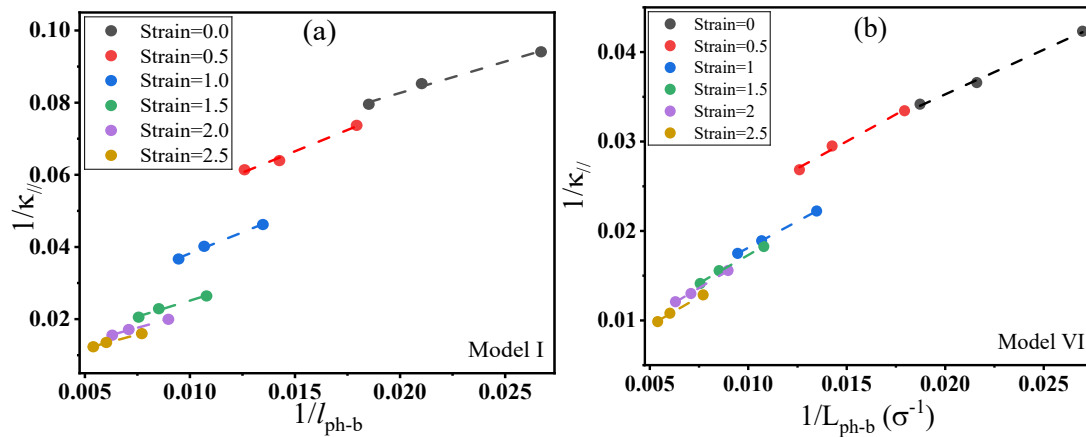


Figure S11. The $1/\kappa_{\parallel}$ vs $1/l_{\text{ph-b}}$ curves as a function of strain for (a) model I ($\chi_c = 0.128$) and (b) model VI ($\chi_c = 0.654$).

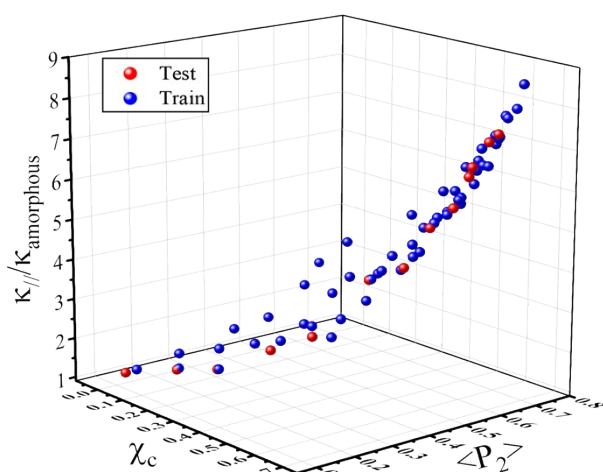


Figure S12. The data set for training model.

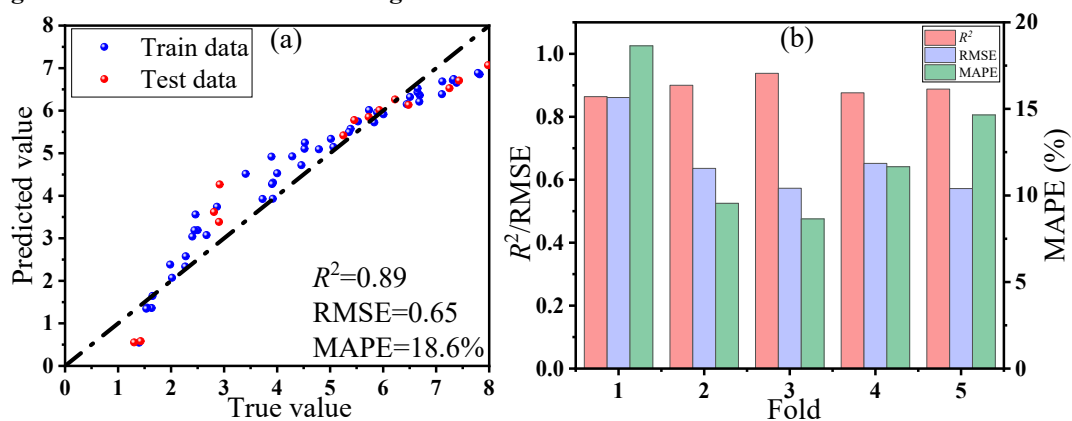


Figure S13. (a) Comparison between the predicted values from LR model and calculated values from MD simulation for the training and test sets, (b) Five-fold cross-validation results in terms of R^2 , RMSE and MAPE.

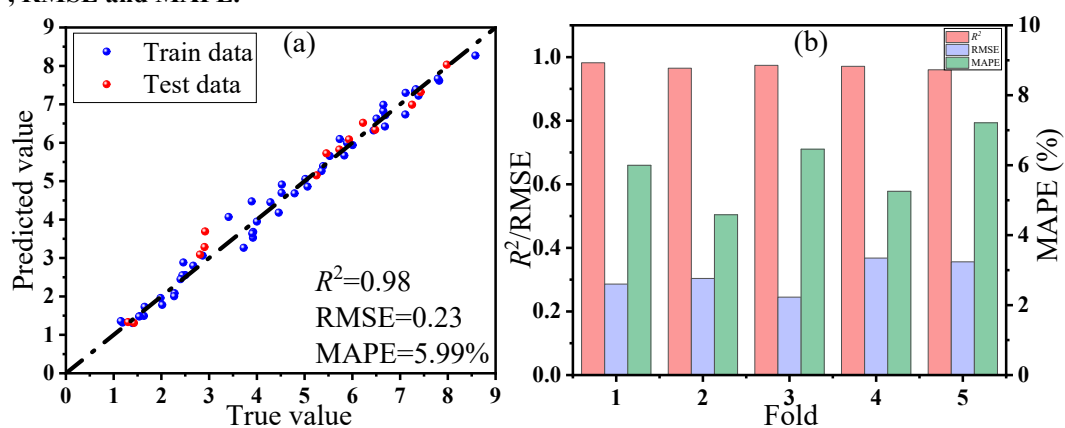


Figure S14. (a) Comparison between the predicted values from PR model and calculated values from MD simulation for the training and test sets, (b) Five-fold cross-validation results in terms of R^2 , RMSE and MAPE.

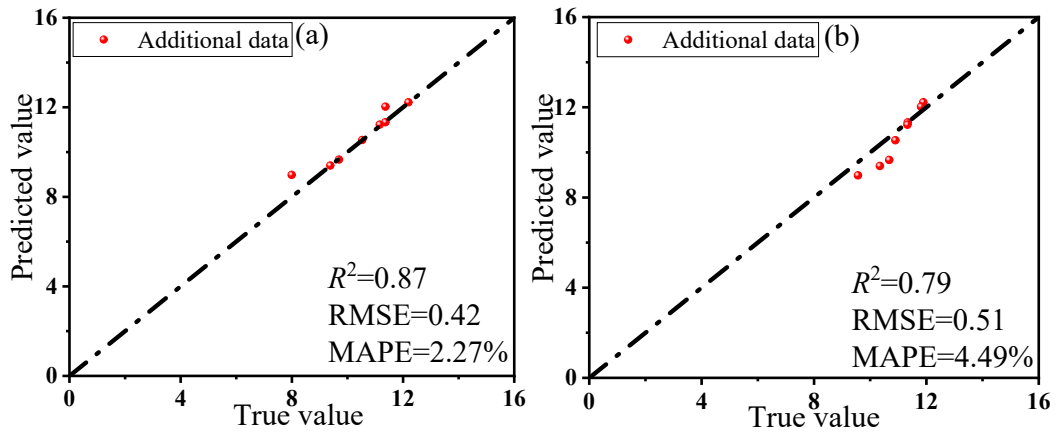


Figure S15. Comparison between the predicted values from (a) XGBoost model and (b) PR model and additional values from MD simulation.

Table SI All the simulation data from MD simulation

Crystallinity (χ_c)	Chain orientation degree ($\langle P_2 \rangle$)	Thermal conductivity ratio ($\kappa_{\parallel} / \kappa_{amorphous}$)
0.653	0.0169	2.90
0.611	0.1804	3.92
0.601	0.3094	3.41
0.621	0.4031	5.06
0.630	0.5020	5.83
0.654	0.5490	6.48
0.662	0.5844	6.69
0.682	0.6165	7.12
0.692	0.6354	7.82
0.712	0.6490	7.98
0.721	0.6613	8.58
0.576	0.0637	2.67
0.543	0.2149	2.81
0.540	0.3443	2.92
0.558	0.4460	3.89
0.582	0.4965	5.02
0.607	0.5449	5.46
0.611	0.5666	6.01
0.643	0.5996	6.51
0.650	0.6121	6.65
0.676	0.6351	7.33
0.688	0.6470	7.79
0.413	0.0120	1.65
0.420	0.1374	2.27

0.423	0.2691	2.40
0.474	0.3697	3.72
0.503	0.4506	4.00
0.550	0.5215	4.52
0.574	0.5503	5.39
0.608	0.5885	5.73
0.628	0.6093	6.22
0.652	0.6272	6.65
0.671	0.6391	7.31
0.265	0.0056	1.30
0.305	0.1062	1.63
0.320	0.2242	2.02
0.407	0.3196	2.50
0.420	0.4089	2.87
0.499	0.4884	4.46
0.520	0.5323	4.79
0.574	0.5834	5.53
0.600	0.5993	5.93
0.633	0.6265	7.11
0.665	0.6339	7.39
0.152	0.0031	1.19
0.188	0.1176	1.43
0.230	0.2125	1.55
0.329	0.3087	2.28
0.395	0.4081	2.46
0.456	0.4694	3.92
0.515	0.5410	4.52
0.546	0.5738	5.35
0.592	0.6004	5.89
0.613	0.6203	6.68
0.665	0.6440	7.43
0.128	-0.0057	1.15
0.185	0.1157	1.40
0.230	0.2080	1.53
0.323	0.2804	1.98
0.370	0.3709	2.44
0.453	0.4660	3.90
0.492	0.5384	4.28
0.537	0.5719	5.25
0.574	0.6048	5.73
0.608	0.6156	6.44
0.648	0.6330	7.25

Table SII Eight additional simulation data from MD simulation

Crystallinity (χ_c)	Chain orientation degree ($\langle P_2 \rangle$)	Thermal conductivity ratio ($\kappa_{\parallel} / \kappa_{amorphous}$)
0.778	0.701	8.98
0.811	0.721	9.40
0.833	0.736	10.5
0.855	0.740	11.3
0.877	0.753	12.2
0.822	0.733	9.66
0.850	0.746	11.2
0.873	0.752	12.0